The Effect of the Wind Farm Construction on Local Thermal Dynamics

Chenzhe Zhang

cz222@duke.edu

December 6, 2025

Abstract

Using Chinese data from 2013–2019, this paper asks whether wind farm construction alters local thermal inversions in ways that threaten the validity of inversion-based instruments for air pollution. We combine annual records on wind farm construction with daily observations from air monitoring stations and estimate dynamic effects using the multiple-period difference-in-differences framework of Callaway and Sant'Anna together with a Double Machine Learning DiD that flexibly controls for high-dimensional weather covariates. Conventional DiD estimates suggest that wind farms broadly reduce inversion probabilities and strength. In contrast, the ML-DiD results indicate that near-surface inversions between layers 1–2 are largely unaffected, whereas higher-layer inversions between layers 3–4 exhibit robust medium-run reductions in inversion probability. These findings imply that low-level inversion measures remain relatively credible instruments, while higher-layer measures may violate the exclusion restriction in regions with intensive wind power deployment.

1 Introduction and Literature Review

There is a large literature on how air pollution affects people's daily lives. Because air pollution and health outcomes are jointly determined by many economic and environmental factors, endogeneity is a central concern. Many scholars therefore rely on instrumental variables. Some studies use thermal inversions as instruments for local air quality (Chen et al., 2018; He et al., 2025; Xia et al., 2022); others exploit pollution transported from upwind cities (Chen et al., 2021; Dai et al., 2024; Fan, 2024) or exogenous shocks such as policy changes (Jiang et al., 2021), the construction of highways(Deryugina et al., 2019), or local terrain and wind patterns (Batkeyev and DeRemer, 2023). Typical control variables include local meteorological conditions such as temperature, wind speed, wind direction, and precipitation.

On the other hand, several studies suggest that the construction of wind farms can also affect local air pollution (Millstein et al., 2017) through the substitution effects by substituting the coal grid electricity, and others document that wind farms may influence health outcomes such as sleep-related problems and annoyance through non-pollution channels like noise and visual intrusion (McCunney et al., 2014; Schmidt and Klokker, 2014; Van Kamp and Van Den Berg, 2021). From this stream of literature, we can argue that the constitutions of the wind farms can be one of the control variables that some previous literature may overlook when choosing the instrument variables. More specifically, the thermal inversion may not satisfy the exclusive condition.

Instrumental variables based on policy shocks, horizontal transport of air pollution, or local terrain are unlikely to be directly affected by the construction of nearby wind farms. By contrast, local thermal inversions may be. A thermal inversion occurs when air temperature increases with height so that the upper layer is warmer than the near-surface layer. Turbine-induced turbulence can enhance vertical mixing and bring warmer air from aloft down toward the ground (Harris et al., 2014). Consequently, the operation of wind farms could plausibly influence the frequency and intensity of local thermal inversions.

Motivated by this physical evidence and the previous literature, we therefore pose the following research question: does the construction of wind farms affect the frequency of thermal inversions? Figure 1 shows the relation between the previous literature, and our potential contribution.

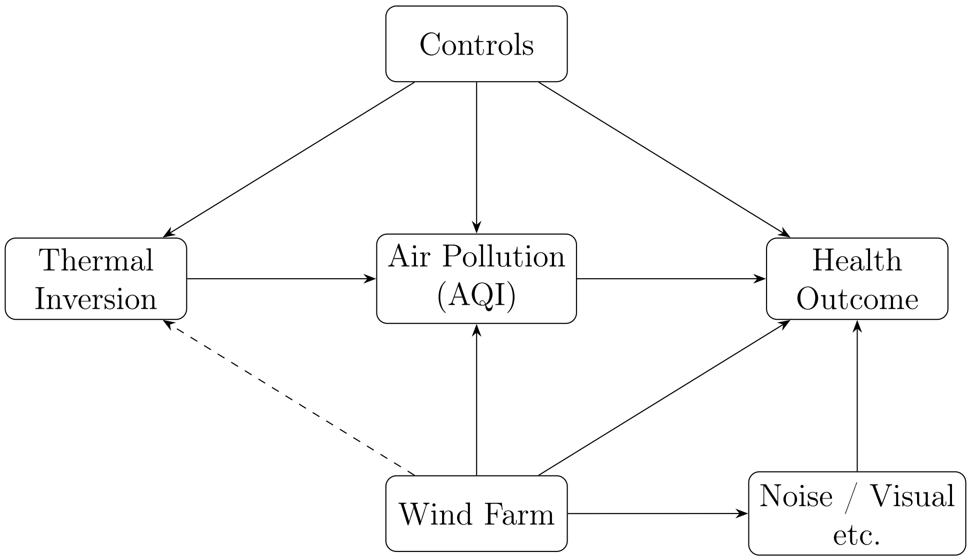

Figure 1: Causal DAG for air pollution, wind farms, thermal inversions and health

2 Methodology

2.1 Data Source

Our dataset combines two main sources. First, we use records on the construction year of Chinese wind farms from the Global Wind Power Tracker Global Energy Monitor (2025). Second, we use daily data on air pollution, thermal inversion frequency, and local meteorological conditions (wind speed, wind direction, temperature, temperature range, and the number of days with precipitation) from air monitoring stations compiled by the Ministry of Ecology and Environment of the People's Republic of China. Thus, our data consist of annual wind farm construction records and daily air-station observations for the period 2013–2019.

We define thermal inversion as the temperature difference between upper and lower layers of the atmosphere,together we have 5 layers. Our daily data record both whether a thermal inversion occurs and the associated temperature difference when it does. Based on this, we construct three annual measures: (i) the average daily thermal inversion frequency, (ii) the average thermal inversion strength (the mean temperature difference on inversion days), and (iii) the annual probability of thermal inversion, defined as the share of days in a year with at least one inversion.

In the raw data, wind speed is reported in 18 categories and wind direction in 7 categories. We list more details in Table 1

Table 1: Summary Statistics

Variable	N	Mean	SD	Min	Median	Max
Panel A: Outcomes						
Thermal Inversion Frequency	9331	0.851	0.326	0.000	0.879	1.658
Thermal Inversion Probability	9331	0.512	0.174	0.000	0.537	0.861
Thermal Inversion Stregthen	9331	0.315	0.187	0.000	0.290	1.177
Panel B: Control Variables						
Average Temperature	9331	15.052	4.709	-0.393	15.948	26.042
Temperature Range	9331	9.422	2.199	4.975	9.008	16.879
Average Precipitation	9331	2.732	1.503	0.007	2.433	9.302
Wind Speed	9331	2.791	10.553	0.000	0.000	303.000
Wind Direction	9331	0.161	1.830	0.000	0.000	52.000

Notes: We have 3 measurements for thermal inversion between two layers; we have 7 categories for the wind direction, and 18 categories for wind speed. For simplicity, we only list some of them. Thermal inversion is for layer 1 and layer 2. Wind direction and wind speed is for the first category.

2.2 Methodology

We estimate the effect of wind-farm construction on local thermal inversions using the multiple-period difference-in-differences framework of Callaway and Sant'Anna (2021). Let $G_i \in \{1, \ldots, T, \infty\}$ denote the first year in which monitoring station i has at least one wind farm constructed within 50km, where $G_i = \infty$ for stations that are never treated during our sample period. Let $Y_{it}(g)$ denote the potential outcome of station i in year t if its first treatment year were g, and let $Y_{it}(\infty)$ denote the potential outcome if it were never treated.

For each cohort g and calendar year $t > g$, the group-time average treatment effect is defined as

$$ATT(g,t) = \mathbb{E}\big[\, Y_t(g) - Y_t(\infty) \;\big|\; G = g \big], \tag{1}$$

where identification relies on a conditional parallel trends assumption between cohort g and the not-yet-treated (including never-treated) stations in year t.

We first estimate $ATT(g,t)$ by comparing stations in cohort g to stations that have not yet been treated in year t. We then aggregate these group-time effects into an event-time parameter that indexes years relative to the first treatment:

$$ATT(\ell) = \sum_{g \in \mathcal{G}_\ell} w_g(\ell)\, ATT\big(g, g+\ell\big), \qquad \ell = t - g, \tag{2}$$

where $\mathcal{G}_\ell$ is the set of treatment cohorts that are observed at relative time ℓ, and $w_g(\ell)$ denotes the weight placed on cohort g at event time ℓ. In our implementation, $w_g(\ell)$ is proportional to the number of treated stations in cohort g that are observed at $g + \ell$:

$$w_g(\ell) = \frac{N_g}{\sum\limits_{h \in \mathcal{G}_\ell} N_h}, \tag{3}$$

where N_g is the number of treated stations in cohort g. This weighting scheme implies that each treated station receives equal weight within a given event time ℓ.

In addition, we relax the parametric linearity assumptions typically imposed in difference-in-differences specifications. Standard implementations often model the outcome and the treatment assignment as linear functions of a small set of covariates. However, the relationship between local meteorological conditions and thermal inversions is likely to be nonlinear, and the same meteorological variables may also affect the probability and timing of wind-farm construction. To flexibly adjust for these potentially high-dimensional confounders, we combine the DiD framework with double/debiased machine learning following Chang (2020); Chernozhukov et al. (2018).

The key idea is to treat the conditional expectations that link outcomes and treatment status to covariates as nuisance functions that can be estimated by machine learning. In a first step, we use flexible ML methods to estimate (i) the conditional expectation of the outcome given meteorological and other controls and (ii) the propensity of treatment (wind-farm construction) given the same controls. We then partial out these estimated nuisance components and estimate the treatment effect using orthogonalized residuals. Because the resulting score is Neyman-orthogonal with respect to the nuisance functions, the second-stage estimator is doubly robust to regularization bias and remains consistent and asymptotically normal even when the first-stage models are estimated with flexible machine-learning algorithms, provided standard rate conditions are satisfied. We view these DML-based estimates as a robustness check that allows for nonlinear and high-dimensional dependence between local meteorological conditions, treatment assignment, and thermal inversions.

For the outcome models, we combine four learners: OLS, a random forest (`ranger`), and two XGBoost specifications with different learning rates and depths. For the treatment models, we use a logistic GLM, XGBoost, and random forest. These learners are aggregated through non-negative least squares stacking with short-stacking and five-fold sample splitting, so that both the outcome and treatment are predicted flexibly from the covariates and only the residual variation enters the DiD step.

Table 2: Treatment Cohorts Distribution

heightGroup	N	Percent
Never Treated (Control)	928	69.617
Cohort 2014	54	4.051
Cohort 2015	106	7.952
Cohort 2016	67	5.026
Cohort 2017	67	5.026
Cohort 2018	52	3.901
Cohort 2019	59	4.426

3 Results

Since we observe five atmospheric layers and construct three inversion measures, we have 30 potential outcome variables. To keep the analysis focused, we report only a subset of these results in the main text and present the remaining specifications in the appendix. Existing studies that use thermal inversions as instruments typically rely on inversion probability between layers 1 and 2, 2 and 3, and 3 and 4 (Chen et al., 2018; Xia et al., 2022), and, in some cases, on inversion strength between layers 1 and 2 (He et al., 2025). We therefore concentrate on these four outcomes in our main results: the inversion probabilities between layers 1–2, 2–3, and 3–4, and the inversion strength between layers 1–2.

Figures 2–5 compare conventional DiD estimates to Double Machine Learning DiD (ML-DiD) estimates for these four outcomes. In each figure, the conventional DiD results appear in the left panel and the ML-DiD results in the right panel.

Figure 2 reports the event-study coefficients for the inversion probability between layers 1 and 2. Under the conventional specification, pre-treatment coefficients are small and not statistically different from zero, while several post-treatment periods show negative coefficients and some later periods are statistically significant. This suggests that, in a conventional DiD, wind farm construction appears to reduce near-surface inversion probability at longer horizons. In the ML-DiD results, the pre-treatment coefficients remain close to zero, and the post-treatment effects are smaller in magnitude and no longer statistically significant at the 95 percent level. Once we flexibly control for local weather conditions, there is little robust evidence that wind farms affect the probaility of thermal inversion between layers 1 and 2.

Figure 3 shows the inversion probability between layers 2 and 3. The conventional DiD estimates again display pre-treatment coefficients near zero, with one pre-period that is marginally significant, and negative post-treatment coefficients that are often significant. The ML-DiD estimates move the pre-treatment coefficients closer to zero and attenuate the post-treatment effects. Some post-treatment years still have negative coefficients, but they are smaller and less precisely estimated than in the conventional specification.

The strongest conventional effects arise for the inversion probability between layers 3 and 4 in Figure 4. In the conventional DiD, coefficients are close to zero before treatment and become increasingly negative after wind farm construction, with several post-treatment periods significantly different from zero. The ML-DiD estimates again show pre-treatment coefficients near zero, which is consistent with the parallel trends assumption, and smaller post-treatment effects. For this specification, however, we still find negative and statistically significant effects in post periods 2 to 4, although the magnitudes are smaller and the pattern is less persistent than in the conventional DiD.

Finally, Figure 5 presents the results for inversion strength between layers 1 and 2. The conventional DiD estimates suggest a modest reduction in strength in later post-treatment years, with some negative and statistically significant coefficients. By contrast, the ML-DiD estimates are close to zero throughout the event window and never statistically significant.

A further difference between the two approaches is that the ML-DiD estimates exhibit larger standard errors and wider confidence intervals than the conventional DiD estimates. This pattern is expected given the design of the estimator. The machine learning step explains a large share of the variation in outcomes and treatment using the covariates, so the residual variation available to identify the treatment effect is smaller and the estimated effects are less extreme. In addition, the use of flexible learners, stacking, and five-fold cross-fitting explicitly propagates the uncertainty from estimating high-dimensional nuisance functions, which leads to more conservative inference. In contrast, the conventional DiD relies on a relatively rigid linear specification. If that specification is misspecified, it may understate the true uncertainty and generate spuriously precise and significant estimates. From this perspective, the wider confidence intervals in the ML-DiD results should be interpreted as evidence of more cautious and robust inference rather than as a weakness of the method.

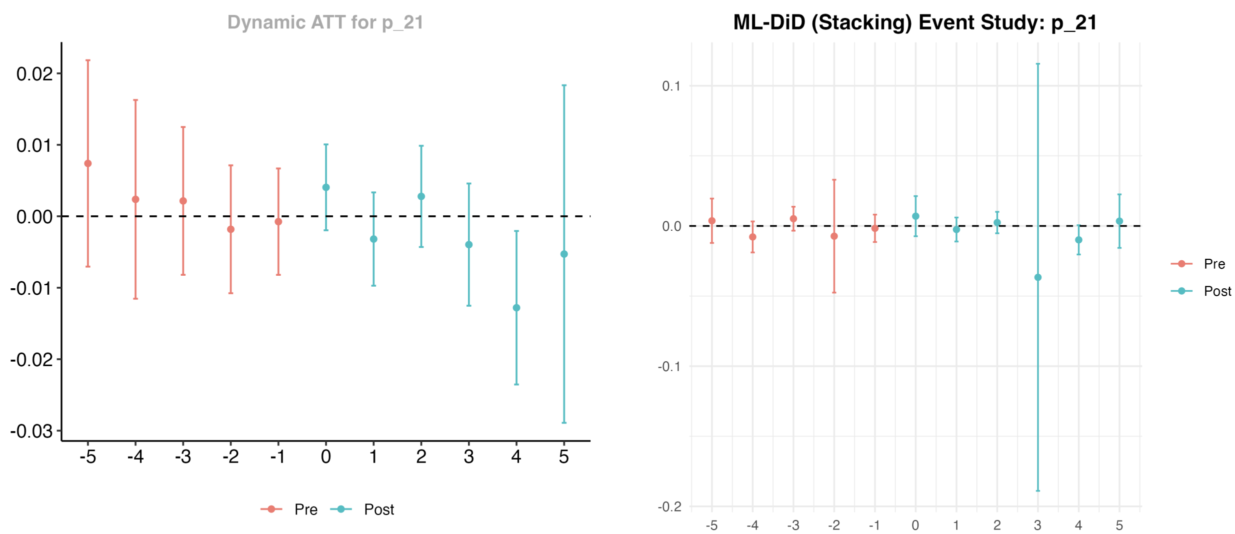

(a) CS DiD Dynamic (b) Robustness MLDiD

Figure 2: Thermal inversion probability between layer 2 and 1

4 Conclusion

This project assesses whether the construction of wind farms affects thermal inversions in ways that may undermine the validity of inversion-based instruments commonly used in air pollution studies. Combining a conventional Callaway–Sant'Anna DiD with a Double Machine Learning DiD, we show that conventional estimates suggest widespread and persistent reductions in inversion probabilities and strength after wind farm construction. Once we flexibly control for high-dimensional and nonlinear weather covariates using ML-DiD, most

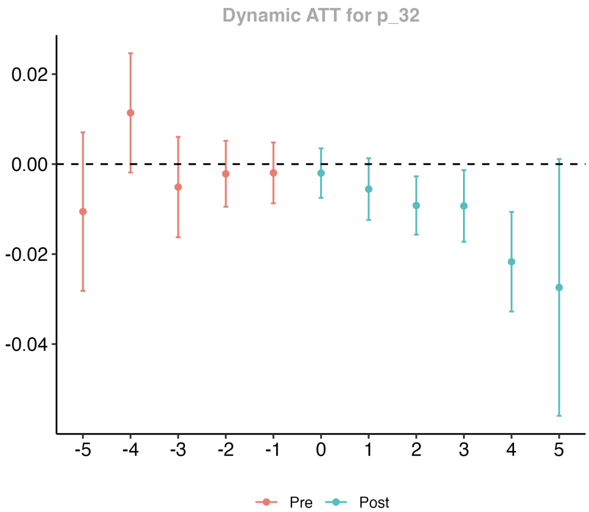

(a) CS DiD Dynamic

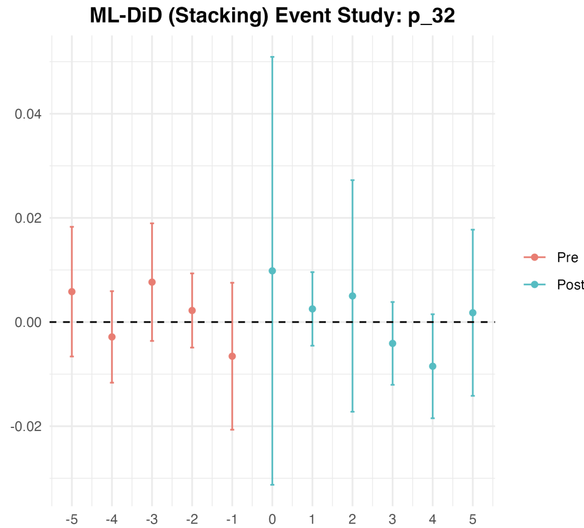

(b) Robustness MLDiD

Figure 3: Thermal inversion probability between layer 3 and 2

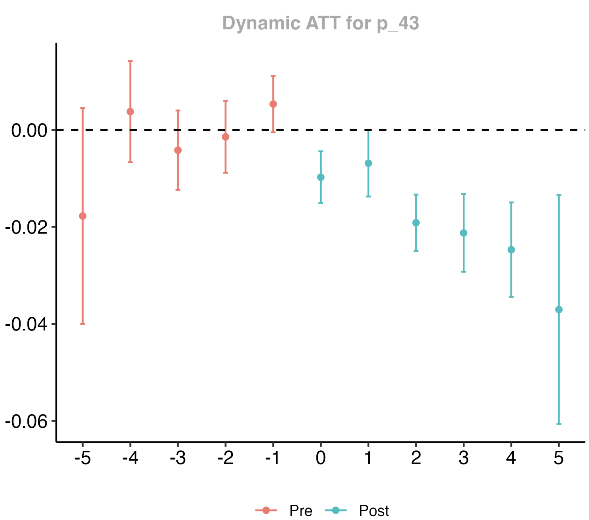

(a) CS DiD Dynamic

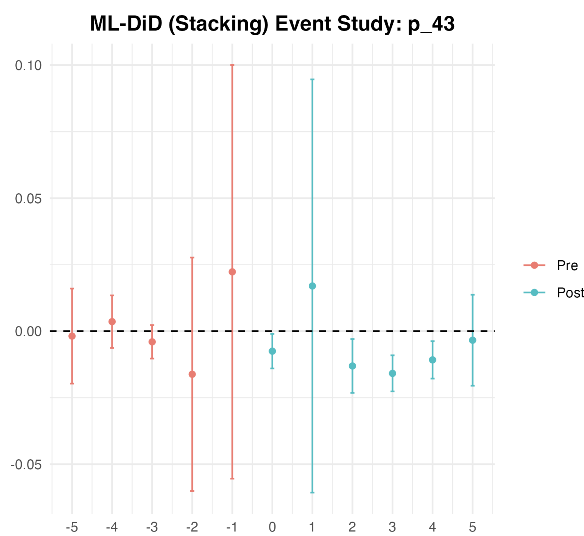

(b) Robustness MLDiD

Figure 4: Thermal inversion probability between layer 4 and 3

Table 3: Dynamic effects of wind farm construction across atmospheric layers and inversion metrics

	Thermal Inversion Probability						Inversion Strength	
	Layers 1–2		Layers 2–3		Layers 3–4		Layers 1–2	
Event Time	CS-DiD	ML-DiD	CS-DiD	ML-DiD	CS-DiD	ML-DiD	CS-DiD	ML-DiD
-5	0.0074	0.0037	-0.0106	0.0058	-0.0178	-0.0018	0.0025	-0.0026
	(0.0051)	(0.0059)	(0.0063)	(0.0051)	(0.0080)	(0.0071)	(0.0073)	(0.0057)
-4	0.0024	-0.0078	0.0114	-0.0029	0.0038	0.0036	0.0063	0.0048
	(0.0049)	(0.0041)	(0.0047)	(0.0036)	(0.0038)	(0.0039)	(0.0056)	(0.0056)
-3	0.0022	0.0052	-0.0051	0.0077	-0.0042	-0.0040	-0.0037	-0.0036
	(0.0037)	(0.0032)	(0.0040)	(0.0046)	(0.0030)	(0.0025)	(0.0044)	(0.0037)
-2	-0.0018	-0.0073	-0.0022	0.0022	-0.0014	-0.0162	-0.0052	-0.0027
	(0.0032)	(0.0149)	(0.0026)	(0.0029)	(0.0027)	(0.0174)	(0.0031)	(0.0032)
-1	-0.0008	-0.0017	-0.0020	-0.0066	0.0053	0.0223	-0.0034	0.0003
	(0.0026)	(0.0036)	(0.0024)	(0.0058)	(0.0021)	(0.0307)	(0.0025)	(0.0027)
0	0.0040	0.0070	-0.0020	0.0098	-0.0098*	-0.0075*	0.0029	0.0008
	(0.0021)	(0.0053)	(0.0020)	(0.0167)	(0.0019)	(0.0026)	(0.0024)	(0.0042)
1	-0.0032	-0.0025	-0.0056	0.0025	-0.0069*	0.0170	-0.0040	-0.0034
	(0.0023)	(0.0032)	(0.0025)	(0.0029)	(0.0025)	(0.0307)	(0.0032)	(0.0032)
2	0.0028	0.0024	-0.0092*	0.0050	-0.0192*	-0.0131*	0.0067	-0.0024
	(0.0025)	(0.0028)	(0.0023)	(0.0091)	(0.0021)	(0.0040)	(0.0034)	(0.0346)
3	-0.0040	-0.0366	-0.0093*	-0.0041	-0.0212*	-0.0159*	0.0007	-0.0418
	(0.0030)	(0.0564)	(0.0029)	(0.0032)	(0.0029)	(0.0027)	(0.0041)	(0.0637)
4	-0.0128*	-0.0099	-0.0217*	-0.0085	-0.0247*	-0.0108*	-0.0165*	-0.0088
	(0.0038)	(0.0039)	(0.0040)	(0.0041)	(0.0035)	(0.0028)	(0.0049)	(0.0053)
5	-0.0053	0.0034	-0.0274	0.0018	-0.0371*	-0.0034	-0.0332	-0.0174
	(0.0084)	(0.0071)	(0.0102)	(0.0065)	(0.0085)	(0.0068)	(0.0128)	(0.0114)

Notes: This table consolidates event-study estimates for the effects of wind farm construction on thermal inversion probabilities (Layers 1–2, 2–3, 3–4) and inversion strength (Layers 1–2).
Coefficients are reported with standard errors in parentheses below. The estimation window covers relative event times from -5 to $+5$ years.
Two specifications are presented for each outcome: the Callaway–Sant'Anna DiD (CS-DiD) and the Double Machine Learning DiD (ML-DiD).
* indicates that the 95% simultaneous confidence band does not cover zero.

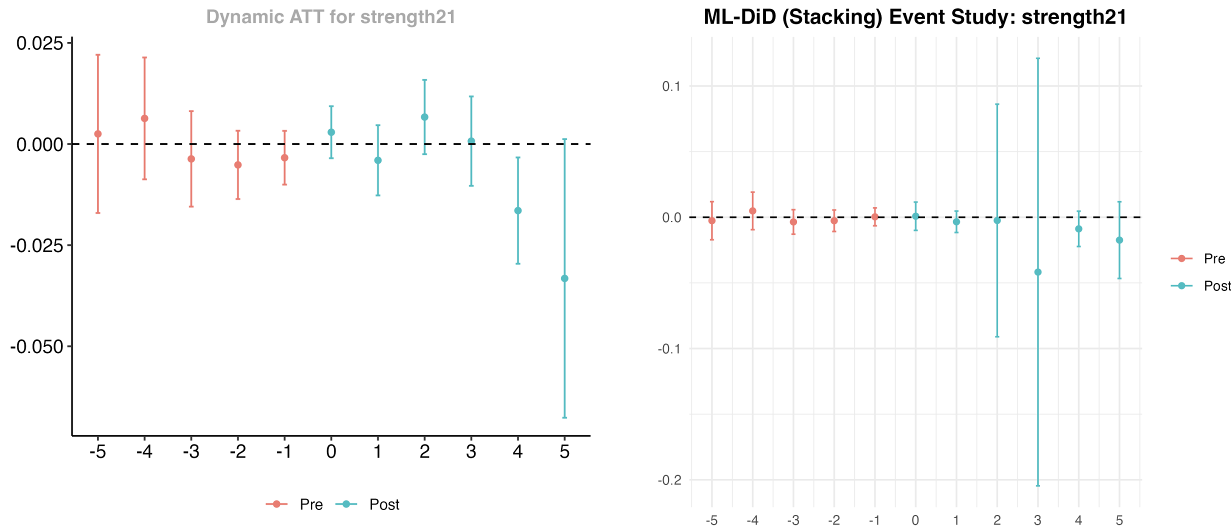

(a) CS DiD Dynamic

(b) Robustness MLDiD

Figure 5: Thermal inversion strength between layer 2 and 1

of these effects become smaller and less precisely estimated. The near-surface inversion measures between layers 1–2 show little robust response to wind farm construction, whereas the inversion probability between layers 3 and 4 exhibits more stable negative effects in the medium run. These findings imply that higher-layer inversion measures may be more problematic as instruments than low-level inversions, especially in regions with intensive wind power deployment.

Our analysis is preliminary and has several limitations. Most importantly, we treat 50 km as an exogenous cutoff to define treated and control air monitoring stations. This threshold is a reasonable starting point but ultimately arbitrary. A more rigorous approach would allow the effect of wind farms to vary continuously with distance and use nonparametric or semi-parametric methods to estimate the distance profile of treatment effects. Future work could also extend the analysis to alternative outcome definitions, longer time periods, and other countries, and more closely link the reduced-form estimates to physical models of how turbines modify local turbulence and vertical heat transfer. Even with these caveats, the evidence presented here suggests that researchers should carefully justify and test the use of thermal inversions as instruments, particularly when relying on higher-layer inversion probabilities.

References

Batkeyev, B. and DeRemer, D. R. (2023). Mountains of evidence: The effects of abnormal air pollution on crime. *Journal of Economic Behavior & Organization*, 210:288–319.

Callaway, B. and Sant'Anna, P. H. (2021). Difference-in-differences with multiple time periods. *Journal of econometrics*, 225(2):200–230.

Chang, N.-C. (2020). Double/debiased machine learning for difference-in-differences models. *The Econometrics Journal*, 23(2):177–191.

Chen, S., Chen, Y., Lei, Z., and Tan-Soo, J.-S. (2021). Chasing clean air: Pollution-induced travels in china. *Journal of the Association of Environmental and Resource Economists*, 8(1):59–89.

Chen, S., Guo, C., and Huang, X. (2018). Air pollution, student health, and school absences: Evidence from china. *Journal of Environmental Economics and Management*, 92:465–497.

Chernozhukov, V., Chetverikov, D., Demirer, M., Duflo, E., Hansen, C., Newey, W., and Robins, J. (2018). Double/debiased machine learning for treatment and structural parameters.

Dai, R., Guo, D., Han, Y., and Qin, Y. (2024). Pollution-induced trips: Evidence from flight and train bookings in china. *Journal of Development Economics*, 171:103340.

Deryugina, T., Heutel, G., Miller, N. H., Molitor, D., and Reif, J. (2019). The mortality and medical costs of air pollution: Evidence from changes in wind direction. *American Economic Review*, 109(12):4178–4219.

Fan, Y. (2024). Social cost of lifestyle adaptation: Air pollution and outdoor physical exercise. *Journal of Environmental Economics and Management*, 127:103042.

Global Energy Monitor (2025). Global wind power tracker. February 2025 release.

Harris, R. A., Zhou, L., and Xia, G. (2014). Satellite observations of wind farm impacts on nocturnal land surface temperature in iowa. *Remote Sensing*, 6(12):12234–12246.

He, G., Pan, Y., and Tanaka, T. (2025). Air pollution and the airborne diseases: Evidence from china and japan. *Journal of Environmental Economics and Management*, 130:103117.

Jiang, X., Li, G., and Fu, W. (2021). Government environmental governance, structural adjustment and air quality: A quasi-natural experiment based on the three-year action plan to win the blue sky defense war. *Journal of Environmental Management*, 277:111470.

McCunney, R. J., Mundt, K. A., Colby, W. D., Dobie, R., Kaliski, K., and Blais, M. (2014). Wind turbines and health: A critical review of the scientific literature. *Journal of Occupational and Environmental Medicine*, 56(11):e108–e130.

Millstein, D., Wiser, R., Bolinger, M., and Barbose, G. (2017). The climate and air-quality benefits of wind and solar power in the united states. *Nature Energy*, 2(9):1–10.

Schmidt, J. H. and Klokker, M. (2014). Health effects related to wind turbine noise exposure: a systematic review. *PloS one*, 9(12):e114183.

Van Kamp, I. and Van Den Berg, F. (2021). Health effects related to wind turbine sound: An update. *International journal of environmental research and public health*, 18(17):9133.

Xia, F., Xing, J., Xu, J., and Pan, X. (2022). The short-term impact of air pollution on medical expenditures: evidence from beijing. *Journal of Environmental Economics and Management*, 114:102680.